

# Set Block Decoding is a Language Model Inference Accelerator

Itai Gat\*, Heli Ben-Hamu\*, Marton Havasi, Daniel Haziza, Jeremy Reizenstein, Gabriel Synnaeve, David Lopez-Paz, Brian Karrer, Yaron Lipman

FAIR at Meta

\*Equal contribution

Autoregressive next token prediction language models offer powerful capabilities but face significant challenges in practical deployment due to the high computational and memory costs of inference, particularly during the decoding stage. We introduce Set Block Decoding (SBD), a simple and flexible paradigm that accelerates generation by integrating standard next token prediction (NTP) and masked token prediction (MATP) within a single architecture. SBD allows the model to sample multiple, not necessarily consecutive, future tokens in parallel, a key distinction from previous acceleration methods. This flexibility allows the use of advanced solvers from the discrete diffusion literature, offering significant speedups without sacrificing accuracy. SBD requires no architectural changes or extra training hyperparameters, maintains compatibility with exact KV-caching, and can be implemented by fine-tuning existing next token prediction models. By fine-tuning Llama-3.1 8B and Qwen-3 8B, we demonstrate that SBD enables a 3-5x reduction in the number of forward passes required for generation while achieving same performance as equivalent NTP training.



## 1 Introduction

Next token prediction (NTP) language models (LMs) have demonstrated extraordinary capabilities across a spectrum of tasks, from natural language understanding to complex reasoning and code generation. These models, built upon the Transformer architecture, have scaled to hundreds of billions and even trillions of parameters, a growth that has been directly correlated with their enhanced performance. However, this large scale presents a challenge for practical deployment. The process of using a trained language model to generate predictions, known as inference or sampling, is both computationally expensive and memory-intensive, creating a significant barrier for real-world applications where low latency and high throughput are important.

Language model inference consists of two parts: the *prefilling* and the *decoding* stages. In the *prefilling* stage, the prompt is processed simultaneously and its attention keys and values (KVs) are cached, which usually achieves a high efficiency on GPUs because thousands of tokens are processed together. In the *decoding* stage, tokens are sequentially generated one after the other and require the attention KVs of preceding tokens: this stage requires few FLOPs per token, yet the entire model weights must be read from GPU memory, along with all cached keys and values, as many times as the number of tokens we want to generate. The decoding stage, which typically dominates the total inference time is the primary focus of many language model optimization efforts. Three main avenues for improvements are: Model compression, system-level optimization, and novel algorithms and modeling.

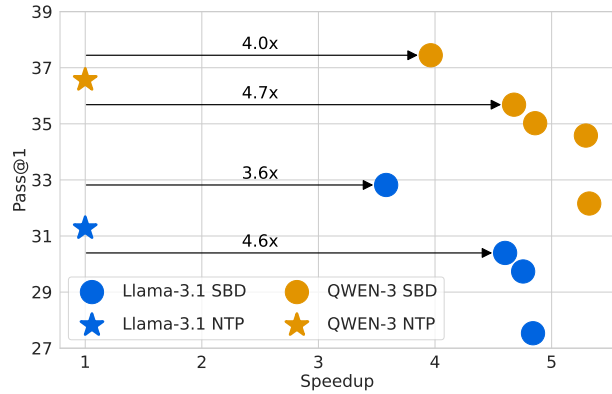


**Figure 1** LiveCodeBench-V6 acceleration with Set Block Decoding with no performance reductions.

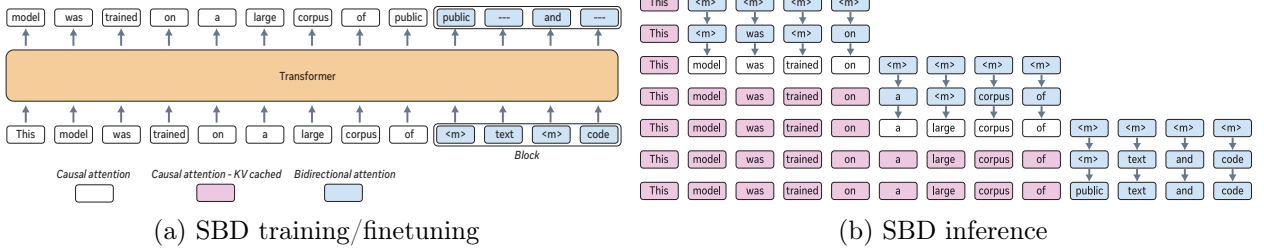


**Figure 2** (a) *Set Block Decoder* fine-tunes any native NTP transformer architecture to predict  $k$  future tokens (in this illustration  $k = 4$ ) conditioned on an arbitrary *subset* of the future tokens (in this case, “text” and “code”); where the special mask token ‘m’ is used to hide future tokens to be predicted. Past tokens (in white) use causal attention while the future block (in blue) uses bidirectional attention, allowing future tokens to attend to each other. (b) During inference, SBD decodes one block at a time by revealing some subset of independent future tokens, where each row represents a single forward in the model. Once a block is decoded it is KV-cached (in pink, with causal attention).

One central approach for accelerating language models within the algorithmic/modeling efforts is *speculative decoding*: generate many tokens with a fast *draft* model and then verify and accept them with the slower *target* model. A smaller language model can be used as the draft model (Leviathan et al., 2023), or additional heads can be attached to the target language model itself to predict multiple independent tokens into the future (Stern et al., 2018; Cai et al., 2024). In both cases the target model is used to verify and accept a consecutive subsequence of these tokens.

The goal of this work is to introduce *Set Block Decoding* (SBD) language models, a flexible and arguably simpler alternative to the draft/target-approach for accelerating language models. SBD models seamlessly combine the standard next token prediction (NTP) paradigm with the masked token prediction (MATP) in the same transformer architecture and, in contrast to previous draft/target-approaches, can sample future tokens in *arbitrary order and in parallel*. This extra degree of freedom unlocks the possibility to employ specialized solvers from the masked diffusion literature, e.g., Ben-Hamu et al. (2025), to achieve significant speedups at no accuracy loss and gain a refined control over the speedup-accuracy tradeoff, see figure 1.

Set Block Decoding models offer the following advantages:

1. *Simplicity*: Single language model, no architectural changes and additions; no added hyper-parameters during training; a single new hyper-parameter during inference.
2. *Flexibility*: Can use advanced solvers from the discrete diffusion literature.
3. *Efficiency*: Compatible with exact KV-caching while offering 3-5x fewer model decoding forwards per generated token.
4. *Computational-cost-effective*: Can be quickly fine-tuned from an existing NTP language model.

Experimentally, we have fine-tuned Llama-3.1 8B and Qwen-3 8B models to make them SBD models and compared to the corresponding NTP baselines trained on the same data and with the same training parameters and noticed that SBD preserve the performance of the NTP models while allows accelerating inference by requiring 3-5x less model forwards.

## 2 Approach

In this section we define SBD models as well as how to train and sample them, see figure 2. For that end, we start with a bit of background on parallel block decoding.

**Notation.** We will mostly follow standard notation denoting a sequence of tokens  $x = (x_1, x_2, \dots, x_L)$ , where  $L$  is the sequence length and each token is an element of a vocabulary set  $x_i \in \mathcal{V} = \{1, 2, \dots, V\}$ . We will use  $\mathcal{I}, \mathcal{J}, \mathcal{T}$  to define sets of indices; accordingly if  $\mathcal{I} = (i_1, \dots, i_m)$  then  $x_{\mathcal{I}} = (x_{i_1}, \dots, x_{i_m})$ .

## 2.1 Parallel block decoding

Large language models generate a sequence of tokens  $x = (x_1, \dots, x_L)$  by repeatedly predicting the next token  $x_t$  given all previous tokens  $x_{<t} = (x_1, \dots, x_{t-2}, x_{t-1})$ ,

$$p(x_t|x_{<t}). \quad (1)$$

This approach is called Next-Token-Prediction (NTP). NTP inference requires one model evaluation per generated token and is therefore slow. *Parallel block decoding* is an attempt to accelerate language models by making them predict  $k$  future tokens (called a *block*) in a single forward pass (Stern et al., 2018),

$$p(x_{\mathcal{I}}|x_{<t}), \quad \mathcal{I} = \{t, t+1, \dots, t+k-1\} \quad (2)$$

where  $x_{\mathcal{I}} = (x_t, x_{t+1}, \dots, x_{t+k-1})$ . However, since modeling the joint probability of more than a single token is intractable with today’s vocabulary sizes  $|\mathcal{V}|$ , e.g., the joint probability mass function of two tokens requires  $|\mathcal{V}|^2$  values in general, previous works resorted to *independent parallel decoding*, that is learning only the *marginals*

$$p(x_i|x_{<t}), \text{ for } i \in \mathcal{I}. \quad (3)$$

Independent parallel decoding provides an independent joint for the future tokens,

$$p(x_{\mathcal{I}}|x_{<t}) = \prod_{i \in \mathcal{I}} p(x_i|x_{<t}), \quad (4)$$

which is in general only a crude approximation to the true joint and therefore requires a verification step that is done with the NTP model and therefore can only accept some consecutive prefix  $x_t, x_{t+1}, \dots, x_{t+a}$ .

## 2.2 Set parallel block decoding

A more general parallel decoding framework is the *set*, or equivalently *mask* parallel decoding (Ghazvininejad et al., 2019; Lou et al., 2023; Gat et al., 2024; Shi et al., 2024; Nie et al., 2025). In a nutshell, Set Block Decoding performs independent parallel decoding of the  $k$  future tokens  $\mathcal{I}$  but allows the model to see an arbitrary *subset*  $\mathcal{J} \subset \mathcal{I}$  of the future tokens. Equivalently, *mask* some of the  $k$  future tokens,  $\mathcal{M} = \mathcal{I} \setminus \mathcal{J}$ , and try to predict the masked tokens,

$$p(x_i|x_{<t}, x_{\mathcal{J}}), \text{ for } i \in \mathcal{M}. \quad (5)$$

This model provides a lot of flexibility in sampling: for any sequence of indices  $\mathcal{I}_1 \subset \mathcal{I}_2 \subset \dots \subset \mathcal{I}_{\ell} = \mathcal{I}$  we can decode all the tokens in  $\mathcal{D}_j = \mathcal{I}_j \setminus \mathcal{I}_{j-1}$  simultaneously leading to

$$p(x_{\mathcal{I}}|x_{<t}) = \prod_{j=1}^{\ell} \prod_{i \in \mathcal{D}_j} p(x_i|x_{<t}, x_{\mathcal{I}_{j-1}}). \quad (6)$$

This sampling will be exact if all  $x_i, i \in \mathcal{D}_j$ , are *conditionally independent*, i.e.,

$$p(x_{\mathcal{D}_j}|x_{<t}, x_{\mathcal{I}_{j-1}}) = \prod_{i \in \mathcal{D}_j} p(x_i|x_{<t}, x_{\mathcal{I}_{j-1}}). \quad (7)$$

This flexibility was recently explored by Ben-Hamu et al. (2025) who suggested a practical algorithm utilizing this principle named *Entropy Bounded* (EB) Sampler. In its simplest form, the EB-Sampler finds at each step a subset of tokens to decode in parallel,  $\mathcal{D}_j$ , by identifying the masked tokens with low *mutual information*, which quantifies the degree of dependence among these tokens. Since the mutual information cannot be computed without the full joint probability, an upper bound is used instead utilizing the entropy of the marginals  $p(x_i|x_{<t}, x_{\mathcal{J}})$ . That is, given we already decoded the tokens corresponding to the indices  $\mathcal{J} \subset \mathcal{I}$  and we are left with masks  $\mathcal{M} = \mathcal{I} \setminus \mathcal{J}$ , we sort the masked token indices,  $\mathcal{M}$ , in ascending order according to entropy of their predicted probabilities, i.e.,  $H(p(x_i|x_{<t}, x_{\mathcal{J}}))$ ; denote the sorted masked indices by  $i_1, i_2, \dots, i_{|\mathcal{M}|}$ . Now, decode in parallel the  $s$  tokens  $i_1, i_2, \dots, i_s$  where  $s \geq 1$  is the largest integer so that

$$\sum_{j=1}^{s-1} H(p(x_{i_j}|x_{<t}, x_{\mathcal{J}})) \leq \gamma, \quad (8)$$

---

**Algorithm 1** Set Block Decoding training

---

**Require:** Init model params  $\theta$ , data  $\mathcal{D}$ .

- 1: **for** data sequence  $x \in \mathcal{D}$  **do**
- 2:   Random noising probability  $\tau \sim U(0, 1)$
- 3:   Create a masked sequence  $\hat{x}$ ; see 13
- 4:   Compute loss  $\mathcal{L}(x, \hat{x}; \theta)$ , see 14
- 5:   Compute gradients and update parameters  $\theta$
- 6: **end for**
- 7: **return**  $\theta$

---

and  $\gamma > 0$  is a user prescribed threshold. At least one token is revealed in each iteration of this algorithm. This algorithm, in contrast to the more classical parallel decoding, can control the efficiency-accuracy tradeoff with the single hyperparameter,  $\gamma$ , and demonstrates impressive reduction in model forwards during sampling. However, translating reductions in model forwards to wall-clock speedups for state-of-the-art autoregressive language models requires combining set parallel decoding with classical next token prediction in a seamless manner. This is what SBD models offer, and this capability is described next.

### 2.3 Set block decoding model

We devise a modeling that allows training of a next token prediction (NTP) model (equation 1) empowered with set block decoding (SBD) abilities (equation 5). The main benefit of SBD models is that they preserve NTP performance while allowing to accelerate inference by using KV-caching and decoding several tokens simultaneously at each step.

An *SBD network* is a transformer  $f_\theta(\cdot; \cdot)$  defined by

$$z_t = f_\theta(x_1, \dots, x_{t-1}; \cdot) \quad (9a)$$

$$(\hat{z}_t, \dots, \hat{z}_{t+k-1}) = f_\theta(x_1, \dots, x_{t-1}; \hat{x}_t, \dots, \hat{x}_{t+k-1}), \quad (9b)$$

where all tokens before (left of) ‘;’ are using causal attention, while tokens after (right of) ‘;’ use bidirectional attention, see figure 3. The “noisy” tokens,  $\hat{x}_t, \dots, \hat{x}_{t+k-1}$ , can be either real tokens from  $\mathcal{V}$  or a mask token denoted ‘m’, i.e.,  $\hat{x}_i \in \mathcal{V} \cup \{m\}$ , for  $i \in \mathcal{I}$ ; see figure 2 (a) for an illustration of  $f_\theta$  for  $k = 4$ .

As usual, each of the logits  $z_t, \hat{z}_t \in \mathbb{R}^V$  define a probability mass function for the generated token  $x_t$  defined via softmax. We consequently denote by

$$p_\theta(x_t | x_{<t}; \cdot) \quad (10)$$

$$p_\theta(x_{t+i} | x_{<t}; \hat{x}_t, \dots, \hat{x}_{t+k-1}), \quad i = 0, \dots, k-1 \quad (11)$$

the probability mass functions defined by the logits  $z_t$  (top equation) and  $\hat{z}_t, \dots, \hat{z}_{t+k-1}$  (bottom equation), respectively.

**Inference with an SBD model.** The SBD model can be sampled with the help of any masked parallel decoding method. We opt for the EB-Sampler where the masked probability in equation 5 is defined using the model as

$$p(x_i | x_{<t}, x_{\mathcal{J}}) = p_\theta(x_i | x_{<t}; \hat{x}_t, \dots, \hat{x}_{t+k-1}), \quad i \in \mathcal{M}, \quad (12)$$

and  $\mathcal{M} \subset \mathcal{I}$  are the masked indices,  $\hat{x}_j = x_j$  if  $j \in \mathcal{J} = \mathcal{I} \setminus \mathcal{M}$  (i.e., unmasked) and  $\hat{x}_j = m$  otherwise. Algorithm 2 provides a sampling pseudo-code, where SAMPLE\_BLOCK is the procedure for sampling the next block and is provided in algorithm 3, utilizing the EB-Sampler (section 2.2); see figure 2 (b) for an illustration of the sampling algorithm with block size  $k = 4$ .

---

**Algorithm 2** Set Block Decoding inference

---

**Require:** Model  $f_\theta$ , prompt  $x_{<0}$ , block size  $k$ , length  $L$

- 1:  $x \leftarrow x_{<0}$
- 2: Prefill  $f_\theta(x)$
- 3: **for**  $t = 0, k, 2k, \dots, L-k$  **do**
- 4:    $x_{<t+k} \leftarrow \text{SAMPLE\_BLOCK}(x_{<t})$
- 5: **end for**
- 6: **return**  $x_{<L}$

---

	$x_1$	$x_2$	$x_3$	...	$x_{t-1}$	$\hat{x}_t$	$\hat{x}_{t+1}$	$\hat{x}_{t+2}$	$\hat{x}_{t+3}$
$x_1$									
$x_2$									
$x_3$									
$\vdots$									
$x_{t-1}$									
$\hat{x}_t$									
$\hat{x}_{t+1}$									
$\hat{x}_{t+2}$									
$\hat{x}_{t+3}$									

**Figure 3** The attention mask of the SBD transformer  $f_\theta$ , equation 9.

**Training an SBD model.** Training the SBD model combines next token prediction and masked prediction losses. In more detail, consider given a sequence of tokens  $x = (x_1, \dots, x_L)$ , we create an additional masked sequence  $\hat{x} = (\hat{x}_1, \dots, \hat{x}_L)$  by setting, for  $i \in [L]$ , where  $[L] = \{1, \dots, L\}$ ,

$$\hat{x}_i = \begin{cases} m & \text{with prob } \eta \\ x_i & \text{with prob } 1 - \eta \end{cases} \quad (13)$$

where  $\eta$  is randomized uniformly in  $(0, 1)$ . Then the *SBD loss* for the sequence  $x$  and block size  $k$  is

$$\mathcal{L}(x, \hat{x}; \theta) = \underbrace{-\sum_{t=2}^L \log p_\theta(x_t | x_{<t};)}_{\text{Next token prediction}} - \underbrace{\sum_{t \in \mathcal{T}} \sum_{i=0}^{k-1} \mathbb{1}_{\hat{x}_{t+i}=m} \log p_\theta(x_{t+i} | x_{<t}; \hat{x}_t, \dots, \hat{x}_{t+k-1})}_{\text{Masked token prediction}} \quad (14)$$

where  $\mathbb{1}_C$  is 1 when condition  $C$  holds and otherwise 0, and  $\mathcal{T} = \{1 + \ell k \mid \ell = 0, 1, 2, \dots, \lfloor \frac{L}{k} \rfloor - 1\}$ . [Algorithm 1](#) provide training pseudo-code, and [figure 2](#) (a) and [figure 8](#) illustrate the training (input, target and attention) for the running example of block size  $k = 4$ .

### 3 Experiments

In this section we report experiments and evaluations of the Set Block Decoding method for accelerating large language models. In [section 3.1](#) we fine-tune two leading 8B models (Llama-3.1 and Qwen-3) and benchmark them on a suite of generation tasks covering reasoning, coding, and mathematics. Next, in [section 3.2](#) we investigate the method’s scaling properties compared to NTP models on smaller, 3B models. We use these experiments to formulate a training recipe for SBD models.

#### 3.1 Benchmarks

**Experimental setup.** We fine-tune Llama-3.1 8B base ([Meta, 2024](#)) and Qwen-3 8B ([Yang et al., 2025a](#)) base models on 70B tokens. We train these models on a mix of reasoning and instruction data with a 32k token context length. The reasoning data mix is composed of mitigated versions of the OpenCodeReasoning ([Ahmad et al., 2025](#)) and OpenMathReasoning ([Moshkov et al., 2025](#)) datasets, where mitigations including algorithmic bias filtering and cybersecurity protections, were applied. For instruct data, we use a publicly available mix, similar to the one used for training Llama-3.1 Instruct. For optimization, we use AdamW ([Loshchilov and Hutter, 2019](#)) with a 3e-4 learning rate, a warmup of 200 iterations, and cosine annealing schedule. We use a batch size of 2M tokens and total 34k iterations of fine-tuning. To support our method, we train models with a variable block size by uniformly sampling a size from the range [2,16] at each training step. At inference, we use EB-Sampler as described in [equation 8](#) with temperature 0.

**Results.** [Table 1](#) presents results for our SBD models on reasoning benchmarks AIME25, LiveCodeBench v6 ([Jain et al., 2024](#)), Math500 ([Lightman et al., 2023](#)), as well as chat benchmarks GSM8K ([Cobbe et al., 2021](#)), HumanEval+ ([Liu et al., 2023](#)), and MBPP ([Austin et al., 2021](#)). For reasoning benchmarks, we generate with thinking and up to 32k tokens; for chat benchmarks we do not use thinking and generate 1024 tokens for HumanEval+ and GSM8K, and 256 for MBPP. The  $\gamma$  values we used for reasoning are  $\gamma_{\text{low}} = 0.1, \gamma_{\text{high}} = 0.35$ ; while for chat benchmarks we use  $\gamma_{\text{low}} = 0.35, \gamma_{\text{high}} = 0.6$ .

To isolate the effect of training data quality on performance and to ensure a fair comparison between SBD and NTP, for each base model we trained an NTP baseline, corresponding to NTP in the loss column in [table 1](#), in the exact same experimental setting and confirmed that the SBD performance is consistent with it.

Base Model	Training	Loss	Sampling	Speedup	Reasoning			Chat		
					MATH500	AIME25	LCB V6	GSM8K	HE+	MBPP
Gemini diffusion	-	-	Diffusion	-	-	23.3	30.9	-	-	76.0
Mercury	-	-	Diffusion	-	-	25.0	-	-	-	76.6
Diffucoder	Scratch	MATP	Diffusion	1x	-	-	-	-	68.3	67.5
Llada 1.5	Scratch	MATP	Diffusion	1x	-	-	-	83.3	52.4	42.8
Dream-coder	FT	MATP	Diffusion	1x	-	-	21.4	-	-	79.6
Llama-3.1 8B	FT	NTP	NTP	1x	80.2	33.3	31.5	85.3	56.7	70.4
		SBD	NTP	1x	81.6	30.0	31.3	85.6	57.9	70.9
		SBD	SBD ( $\gamma_{\text{high}}$ )	3.4x	80.4 (3.23x)	23.3 (4.50x)	29.9 (4.59x)	84.0 (2.34x)	54.9 (2.05x)	67.2 (2.66x)
		SBD	SBD ( $\gamma_{\text{low}}$ )	3.0x	81.0 (3.55x)	30.0 (3.35x)	31.7 (3.72x)	84.2 (2.20x)	57.9 (2.61x)	69.5 (2.49x)
Qwen-3 8B	FT	NTP	NTP	1x	86.6	33.3	36.6	90.1	69.5	78.0
		SBD	NTP	1x	86.6	33.3	37.4	90.4	66.5	77.7
		SBD	SBD ( $\gamma_{\text{high}}$ )	3.8x	85.4 (3.54x)	26.6 (5.06x)	33.3 (5.36x)	88.7 (2.86x)	65.2 (2.72x)	74.6 (3.03x)
		SBD	SBD ( $\gamma_{\text{low}}$ )	3.2x	85.0 (3.41x)	33.3 (3.85x)	37.2 (3.92x)	90.1 (2.77x)	66.5 (2.51x)	77.5 (2.61x)

**Table 1** Reasoning, coding, and math benchmark results. All baselines use greedy decoding. SBD models are sampled with a fixed entropy threshold and two  $\gamma$  settings: a low value that preserves accuracy and a high value that prioritizes speed. Speedup is measured as the reduction in NFEs (model forwards); see section 4 for the wall-clock time analysis.

We find that for low  $\gamma$  values, our method preserves the autoregressive performance while achieving a 3-5x speedup (benchmark-dependent) and higher  $\gamma$  values yield even greater speedups at the cost of a minor drop in performance. Figure 1 illustrates the tradeoff between speed and performance when tweaking the  $\gamma$  threshold of the EB-Sampler.

*In all benchmarks, similar to the “generate until” logic presented in Ben-Hamu et al. (2025), we measure speedup only until the end of the problem’s solution.*

### 3.2 Ablations

**Experimental setup.** For all experiments in this section we use a 3B transformer model, with 28 layers, and a hidden dimension of 3072. For pretraining experiments, we use AdamW with a peak learning rate of 1.5e-3, warmup of 2000 steps and a cosine annealing schedule, for a total of 1T tokens from a mitigated version of DCLM (Li et al., 2024a) and raw code data. For instruct SBD fine-tuning, we use AdamW with a peak learning rate of 1e-5, warmup of 200 steps and a cosine annealing schedule. We train with the same instruct data used in section 3.1.

**Role of NTP loss term.** We assess the significance of the NTP loss term (see equation 14) by training two variants: standard SBD, and a variant where we do not take gradients over the NTP term, but we do log its values during training. Both variants begin from the same intermediate training step, namely the 900B checkpoint of a standard NTP model pre-training. We train SBD with and without the NTP term for the remaining 100B tokens, continuing with the same exact optimization hyperparameters as the NTP training.

Figure 4 shows the NTP loss during training in three configurations: (i) standard NTP model training (gray), (ii) SBD training (orange), and (iii) SBD training w/o NTP term (blue). One can see that without the NTP loss term, SBD training will not maintain the AR capabilities of the base model, while training SBD with the full loss only results in a slightly higher NTP loss.

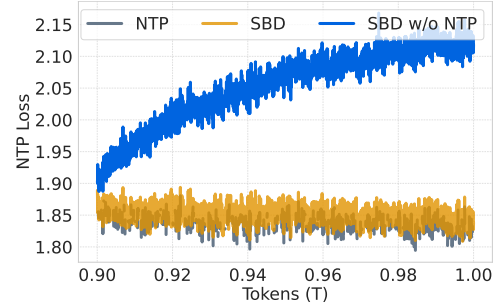


**Figure 4** NTP loss during 3B model pretraining.

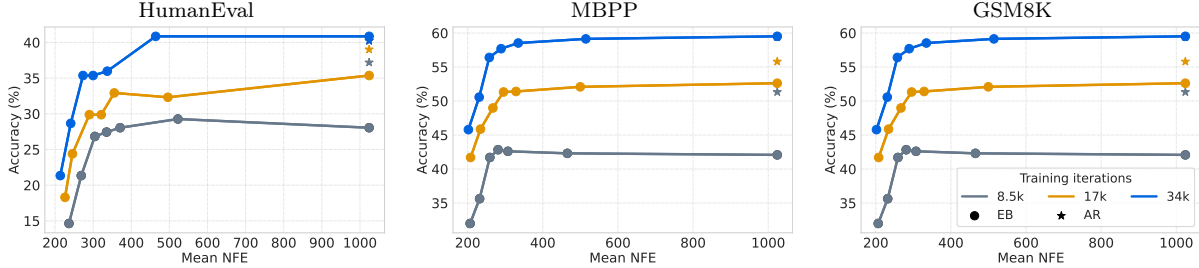


**Figure 5** 3B model SFT training with varying number of training iterations.

	MMLU	GPQA	Hellaswag	Winogrande	ARC-E	ARC-C
NTP	50.9	24.1	76.4	69.5	71.2	51.4
SBD	49.9 <small>-1.0%</small>	27.7 <small>+3.6%</small>	75.6 <small>-0.8%</small>	70.2 <small>+0.7%</small>	69.9 <small>-1.3%</small>	48.6 <small>-2.8%</small>
SBD w/o NTP loss	43.2 <small>-7.7%</small>	27.2 <small>+3.1%</small>	71.1 <small>-5.2%</small>	67.2 <small>-2.2%</small>	58.8 <small>-12.4%</small>	43.2 <small>-8.2%</small>

**Table 2** Ablation on 3B-parameters pretrained models trained on 1T tokens. SBD models start from an intermediate training step of the NTP pretrained model and are trained for the last 10% of the tokens. The difference in accuracy compared to the NTP baseline is listed in subscript for the SBD models.

[Table 2](#) further validates the observed behavior in [figure 4](#) by evaluating the models on likelihood tasks: MMLU ([Hendrycks et al., 2021](#)), GPQA ([Rein et al., 2023](#)), Hellaswag ([Zellers et al., 2019](#)), Winogrande ([Sakaguchi et al., 2019](#)), Arc-E and ARC-C ([Clark et al., 2018](#)), showing significant decrease in accuracy when the NTP loss term is removed compared to full SBD training loss. For the SBD models, inference is done using the NTP prediction as in [equation 9a](#).

**Number of training steps.** State-of-the-art language models are first fully pretrained and then undergo a supervised fine-tuning (SFT) in order to adjust them for specific use cases (e.g., instruct models). The SFT stage is typically significantly shorter than the full pretraining stage and is one of the most common post-training procedures. In this experiment we show SBD can be incorporated effectively into the SFT stage. That is, given a pretrained model, perform SFT with the SBD training scheme. We use the same instruct data used in [section 3.1](#) and the same training hyperparameters for both NTP and SBD fine-tuning. [Figure 5](#) shows SFT models’ performance for both NTP training and SBD training at 1024 generation length, for varying number of training iterations. We observe that SBD requires more steps to reach on-par performance as NTP training but closes the performance gap after roughly 34k training iterations. We also show the performance of the SBD models for different EB-Sampler  $\gamma$  values in  $\{0, 0.01, 0.1, 0.2, 0.4, 0.8, 1.5\}$ . This demonstrates that the EB-Sampler’s behavior, providing speed up at no accuracy loss, as shown in [Ben-Hamu et al. \(2025\)](#) for masked models, translates to the SBD paradigm. In [appendix B.1](#) we also show comparison to the factor sampling algorithm introduced in [Wu et al. \(2025a\)](#).

## 4 Timing analysis

### 4.1 Roofline model for block inference

Standard NTP models perform  $L$  forwards to generate a sequence of length  $L$ . In contrast, SBD models reduce this number of model forwards by a factor of 3-5x (see factors in [table 1](#)) but each forward simultaneously computes a block of  $k$  tokens. In this section we provide a theoretical (“roofline”) analysis to justify why these model forward saving are expected to translate to almost identical factors of wall-clock savings in practice.

Our model assumes the H100 Nvidia GPU and standard 8B transformer model with the following parameters:

```

1 # --- H100 GPU Specifications ---
2 BYTES: int = 1 # model weights, we assume FP8
3 PEAK_FLOPS: float = 1978 * 1e12 # peak flops for FP8
4 PEAK_FLOPS_ATTENTION: float = 989 * 1e12 # attention is done in BF16
5 MEMORY_BANDWIDTH: float = 3.35 * (1024**4) # memory bandwidth in B/s
6
7 # --- Transformer Model Configuration ---
8 HIDDEN_DIM: int = 4096
9 FFN_DIM: int = 4 * HIDDEN_DIM
10 NUM_HEADS: int = 32
11 HEAD_DIM: int = HIDDEN_DIM // NUM_HEADS
12 NUM_KV_HEADS: int = 8
13 BYTES_PER_KV_ELEMENT: float = 1 # bytes used per KV element

```

**Figure 6** Constants for roofline analysis.

The `PEAK_FLOPS` defines the maximal flops/sec for FP8 in H100 while `MEMORY_BANDWIDTH` is the maximal bytes/sec. The main equation to determine the theoretical time of an operation is to take the max upon memory transfers time and compute time via

$$\text{theoretical\_time} = \max \left\{ \frac{\text{total\_flops}}{\text{PEAK\_FLOPS}}, \frac{\text{total\_memory}}{\text{MEMORY\_BANDWIDTH}} \right\}. \quad (15)$$

If the maximum is achieved by the memory part then the computation is called *memory bound* and otherwise it is named *compute bound* ([Williams et al., 2008](#)).

To compare standard NTP and SBD decoding time we analyze different KV Cache lengths, supporting different stages of the generation process with potentially long generation sequences, different sizes of block sizes  $\{1, 2, 4, 8, 16, 32, 64\}$ , where block size of 1 corresponds to NTP sampling and serves as baseline, and batch size, `batch_size`  $\in \{1, 4, 8, 16\}$ . To analyze the theoretical forward time of a transformer we sum the theoretical times of its two components, namely the multi-head attention operation and linear layer. For the attention, we assume a single fused kernel like in [Dao et al. \(2022\)](#). In the appendix, we provide Python code to calculate these theoretical runtimes ([figure 11](#)). [Table 3](#) shows the slowdowns, i.e., the theoretical time ratios, of block sampling and NTP sampling for different block and batch sizes and KV cache length. For example, for block size of 16, the block inference slowdown over NTP is not more than few percents. In the next section, we use this analysis to provide theoretical wall-clock saving times for different NFE speedups.

### 4.2 Set block decoding theoretical speedups

Consider sampling a block of  $k$  tokens from the model. We want to estimate the wall-clock speedup of SBD sampling over NTP. Recall the SBD inference procedure in [algorithm 2](#), which is illustrated in [figure 2](#) (b), and assume that the SBD sampling uses  $l$  model forwards ( $l < k$ ). Then the wall-clock speedup will be the ratio

$$\text{speedup}(l, k) = \frac{k \text{ time}(1)}{\text{time}(2k) + (l - 1)\text{time}(k)}, \quad (16)$$

where  $\text{time}(k)$  is the forward time of a block of size  $k$  in the network.

KV Cache Length	Block Size						
	1	2	4	8	16	32	64
$2^4$ (16)	1.000	1.000	1.001	1.002	1.004	1.008	1.015
$2^8$ (256)	1.000	1.000	1.001	1.002	1.004	1.008	1.015
$2^{10}$ (1,024)	1.000	1.000	1.001	1.002	1.004	1.008	1.015
$2^{12}$ (4,096)	1.000	1.000	1.001	1.002	1.004	1.008	1.015
$2^{14}$ (16,384)	1.000	1.000	1.001	1.002	1.004	1.008	1.015
$2^{16}$ (65,536)	1.000	1.000	1.001	1.002	1.004	1.008	1.016
$2^{20}$ (1,048,576)	1.000	1.000	1.001	1.002	1.004	1.008	1.019
$2^{22}$ (4,194,304)	1.000	1.000	1.001	1.002	1.004	1.007	1.029
<b>batch_size=1</b>							
KV Cache Length	Block Size						
	1	2	4	8	16	32	64
$2^4$ (16)	1.000	1.002	1.006	1.014	1.029	1.060	1.903
$2^8$ (256)	1.000	1.002	1.006	1.014	1.029	1.060	1.903
$2^{10}$ (1,024)	1.000	1.002	1.006	1.014	1.029	1.060	1.903
$2^{12}$ (4,096)	1.000	1.002	1.006	1.014	1.029	1.060	1.903
$2^{14}$ (16,384)	1.000	1.002	1.006	1.014	1.029	1.060	1.903
$2^{16}$ (65,536)	1.000	1.002	1.006	1.014	1.029	1.060	1.903
$2^{20}$ (1,048,576)	1.000	1.002	1.006	1.013	1.028	1.059	1.903
$2^{22}$ (4,194,304)	1.000	1.002	1.005	1.012	1.026	1.054	1.904
<b>batch_size=8</b>							
KV Cache Length	Block Size						
	1	2	4	8	16	32	64
$2^4$ (16)	1.000	1.004	1.012	1.027	1.058	1.899	3.799
$2^8$ (256)	1.000	1.004	1.012	1.027	1.058	1.899	3.799
$2^{10}$ (1,024)	1.000	1.004	1.012	1.027	1.058	1.899	3.799
$2^{12}$ (4,096)	1.000	1.004	1.012	1.027	1.058	1.899	3.798
$2^{14}$ (16,384)	1.000	1.004	1.012	1.027	1.058	1.899	3.797
$2^{16}$ (65,536)	1.000	1.004	1.012	1.027	1.058	1.896	3.792
$2^{20}$ (1,048,576)	1.000	1.004	1.011	1.026	1.055	1.847	3.688
$2^{22}$ (4,194,304)	1.000	1.003	1.009	1.022	1.047	1.720	3.422
<b>batch_size=16</b>							

**Table 3** Slowdown factors of a single block forward (for different batch and block sizes and KV cache lengths) compared to a single token forward used in standard NTP sampling, according to theoretical “Roofline” analysis for an H100 NVIDIA GPU and a standard 8B transformer architecture. Uncolored cells exhibit small slowdown. *Note: no NFE speedup is considered here.*

To estimate these times, we will use the roofline analysis from [section 4](#). [Table 4](#) depicts  $\text{speedup}(l, k)$  for different batch and block sizes, KV cache length and

$$\text{NFE\_speedup} = \frac{k}{l}. \quad (17)$$

Note that for block size 16 the NFE speedups translate almost directly to theoretical wall-clock speedups, which covers the experimental setting and provides an evidence for potential 3-5x wall-clock speedup given the NFE speedups in [table 1](#). Lastly, we note that as batch sizes and/or block size increase the roofline analysis indicates diminishing returns due to increased computational costs of block forwards (see colored cells).

## 5 Related work

Efficient large language modeling is a large topic that we do not attempt to cover comprehensively. Instead we summarize research that is most connected to SBD, describing recent diffusion language models as well as related efficiency efforts. Like SBD, this research proposes higher efficiency via computationally cheaper and fewer model evaluations, e.g., applying key-value caching, fusing sequential operations as in tree attention, and parallel decoding. We conclude by discussing hybrid language models.

**Diffusion language models using masked discrete diffusion.** Large language modeling via diffusion at the several billion (or larger) parameter scale has only recently become successful with models such as Dream ([Wu et al., 2025b](#); [Xie et al., 2025](#)), LLaDa ([You et al., 2025](#); [Liu et al., 2025a](#)), MMaDa ([Yang et al., 2025b](#)), Dimple ([Yu et al., 2025](#)), Mercury ([Labs et al., 2025](#)), DiffuCoder ([Gong et al., 2025](#)), Seed Diffusion ([Song et al., 2025](#)), and Gemini Diffusion ([Deepmind, 2025](#)). Prior to the arrival of these masked diffusion models, discrete diffusion for text had been mostly limited to smaller scales. These masked diffusion models are competitive with traditional autoregressive language models on task performance, but are still lacking on end-to-end efficiency, outside commercially developed models, such as Mercury, Seed Diffusion, and Gemini Diffusion, whose inner workings are undisclosed.

**Efficient large language models with causal attention.** Typical language models are autoregressive with a fixed left-to-right order and leverage Transformers using causal attention, enabling the reuse of model computation via key-value caching. This caching is crucial for efficient sampling from these models. Greedy decoding ([Stern et al., 2018](#)) and non-greedy speculative sampling ([Chen et al., 2023](#); [Leviathan et al.,](#)

KV Cache Length		Block Size			
		8	16	32	64
$2^4$ (16)		1.996	1.992	1.984	1.969
$2^8$ (256)		1.996	1.992	1.984	1.969
$2^{10}$ (1,024)		1.996	1.992	1.984	1.969
$2^{12}$ (4,096)		1.996	1.992	1.984	1.969
$2^{14}$ (16,384)		1.996	1.992	1.984	1.969
$2^{16}$ (65,536)		1.996	1.992	1.984	1.968
$2^{20}$ (1,048,576)		1.996	1.992	1.984	1.962
$2^{22}$ (4,194,304)		1.996	1.992	1.983	1.941
<b>batch_size=1, NFE_speedup=2</b>					
KV Cache Length		Block Size			
		8	16	32	64
$2^4$ (16)		3.989	3.982	3.966	3.936
$2^8$ (256)		3.989	3.982	3.966	3.936
$2^{10}$ (1,024)		3.989	3.982	3.966	3.936
$2^{12}$ (4,096)		3.989	3.982	3.966	3.936
$2^{14}$ (16,384)		3.989	3.982	3.966	3.935
$2^{16}$ (65,536)		3.989	3.982	3.966	3.935
$2^{20}$ (1,048,576)		3.989	3.982	3.965	3.920
$2^{22}$ (4,194,304)		3.989	3.982	3.960	3.876
<b>batch_size=1, NFE_speedup=4</b>					
KV Cache Length		Block Size			
		8	16	32	64
$2^4$ (16)		7.971	7.955	7.925	7.864
$2^8$ (256)		7.971	7.955	7.925	7.864
$2^{10}$ (1,024)		7.971	7.955	7.925	7.864
$2^{12}$ (4,096)		7.971	7.955	7.925	7.864
$2^{14}$ (16,384)		7.971	7.955	7.924	7.863
$2^{16}$ (65,536)		7.971	7.955	7.924	7.862
$2^{20}$ (1,048,576)		7.971	7.956	7.918	7.830
$2^{22}$ (4,194,304)		7.971	7.956	7.898	7.732
<b>batch_size=1, NFE_speedup=8</b>					
KV Cache Length		Block Size			
		8	16	32	64
$2^4$ (16)		7.885	7.824	7.707	6.856
$2^8$ (256)		7.885	7.824	7.707	6.856
$2^{10}$ (1,024)		7.885	7.824	7.707	6.856
$2^{12}$ (4,096)		7.885	7.824	7.707	6.855
$2^{14}$ (16,384)		7.885	7.824	7.706	6.854
$2^{16}$ (65,536)		7.885	7.825	7.705	6.850
$2^{20}$ (1,048,576)		7.886	7.827	7.685	6.768
$2^{22}$ (4,194,304)		7.891	7.834	7.625	6.534
<b>batch_size=4, NFE_speedup=2</b>					
KV Cache Length		Block Size			
		8	16	32	64
$2^4$ (16)		1.983	1.967	1.938	1.839
$2^8$ (256)		1.983	1.967	1.938	1.839
$2^{10}$ (1,024)		1.983	1.967	1.938	1.838
$2^{12}$ (4,096)		1.983	1.967	1.938	1.838
$2^{14}$ (16,384)		1.983	1.967	1.938	1.838
$2^{16}$ (65,536)		1.983	1.967	1.938	1.837
$2^{20}$ (1,048,576)		1.983	1.968	1.937	1.816
$2^{22}$ (4,194,304)		1.984	1.969	1.935	1.755
<b>batch_size=4, NFE_speedup=4</b>					
KV Cache Length		Block Size			
		8	16	32	64
$2^4$ (16)		3.958	3.927	3.868	3.590
$2^8$ (256)		3.958	3.927	3.868	3.590
$2^{10}$ (1,024)		3.958	3.927	3.868	3.590
$2^{12}$ (4,096)		3.958	3.927	3.868	3.590
$2^{14}$ (16,384)		3.958	3.927	3.868	3.589
$2^{16}$ (65,536)		3.958	3.927	3.868	3.587
$2^{20}$ (1,048,576)		3.958	3.928	3.863	3.545
$2^{22}$ (4,194,304)		3.960	3.931	3.851	3.425
<b>batch_size=8, NFE_speedup=2</b>					
KV Cache Length		Block Size			
		8	16	32	64
$2^4$ (16)		3.916	3.857	3.431	1.978
$2^8$ (256)		3.916	3.857	3.431	1.978
$2^{10}$ (1,024)		3.916	3.857	3.431	1.978
$2^{12}$ (4,096)		3.916	3.857	3.431	1.978
$2^{14}$ (16,384)		3.916	3.857	3.431	1.978
$2^{16}$ (65,536)		3.916	3.857	3.431	1.978
$2^{20}$ (1,048,576)		3.918	3.861	3.436	1.978
$2^{22}$ (4,194,304)		3.925	3.872	3.448	1.978
<b>batch_size=8, NFE_speedup=4</b>					
KV Cache Length		Block Size			
		8	16	32	64
$2^4$ (16)		7.773	7.657	6.294	3.736
$2^8$ (256)		7.773	7.657	6.294	3.736
$2^{10}$ (1,024)		7.773	7.657	6.294	3.736
$2^{12}$ (4,096)		7.773	7.657	6.294	3.736
$2^{14}$ (16,384)		7.773	7.657	6.294	3.736
$2^{16}$ (65,536)		7.773	7.657	6.294	3.736
$2^{20}$ (1,048,576)		7.779	7.667	6.300	3.736
$2^{22}$ (4,194,304)		7.797	7.693	6.318	3.736
<b>batch_size=8, NFE_speedup=8</b>					

**Table 4** Theoretical wall-clock speedups of block decoding compared to standard NTP sampling for different NFE speedups based on roofline analysis. Uncolored cells exhibit wall-clock speedup roughly equivalent to NFE speedup.

2023) can improve efficiency further, by proposing candidate sequences from a cheap draft model and only evaluating those candidates with the NTP language model. For example, text diffusion was proposed as a draft in Christopher et al. (2025). Because multiple models adds system complexity, approaches such as multi-token prediction (Gloeckle et al., 2024), Medusa (Cai et al., 2024), and Eagle (Li et al., 2024b), add output heads to an existing language model to predict consecutive future tokens. This multi-head prediction enables self-speculative decoding without a separate draft. Unlike our approach, these methods require adding architectural constructions which introduce a tradeoff challenge and a large to explore hyperparameter space. Any-order autoregressive models (Uria et al., 2014; Hoogeboom et al., 2022) discards the left-to-right order but maintains causal attention and exact key-value caches, and have similar draft variants (Pannatier et al., 2024; Guo and Ermon, 2025).

**Efficient diffusion language models with bidirectional attention.** As strongly performing masked diffusion models are recent, efficient sampling is even more recent and has focused on improvements to LLaDa and Dream. This research has introduced approximate key-value caching (Ma et al., 2025; Liu et al., 2025b) and adaptive multi-token sampling (Ben-Hamu et al., 2025), and explored both avenues simultaneously (Wu et al., 2025a; Hu et al., 2025; Israel et al., 2025). Exact key-value caching is not possible with bidirectional attention, and heuristic approximations rely upon utilizing empirical observations of slowly changing representations, especially for mask tokens. On the sampling side, (Ben-Hamu et al., 2025; Wu et al., 2025a) propose non-greedy and greedy decoding schemes designed to control error from parallel multi-token sampling, while Hu et al. (2025); Israel et al. (2025) consider leveraging autoregressive model outputs to correct for independent unmasking. Unmasking orders are often constrained, with semi-autoregressive blockwise decoding used in Wu et al. (2025a); Hu et al. (2025) and even left-to-right decoding suggested (Israel et al., 2025).

**Hybrid language models.** Most related to SBD are recent proposals to mix left-to-right and parallel modeling. Block diffusion (BD3-LM) (Ariola et al., 2025), proposes semi-autoregressive generation within blocks, uses block-causal attention and exact key-value caching for preceding blocks, proposes unmasking tokens within a block using diffusion and bidirectional attention. CtrlDiff built upon BD3-LM adding adaptive

block size selection (Huang and Tang, 2025). Fathi et al. (2025) concurrently built upon BD3-LM to combine NTP and block diffusion, however with the goal of testing hybrid probability paths with a mix of uniform and masked noising process for improving performance at the cost of longer inference. Finally Esoteric Language Models (Sahoo et al., 2025), claim to improve upon BD3-LM, by considering a hybrid construction that uses bidirectional attention over clean tokens and causal attention over masked tokens to enable KV-caching. While these methods focus on a similar goal, fusing NTP with MATP models, our work introduces an efficient method to fine-tune an existing NTP model, taking advantage of the efficient NTP training, while providing it with the ability for fast block decoding; this allows us to gain a 3-5x speedup without altering the model architecture or compromising its performance.

## 6 Conclusion and future work

This work introduces Set Block Decoding (SBD), a simple and effective paradigm for accelerating the inference of large language models. By integrating masked-token prediction directly into a standard autoregressive architecture, SBD models can decode multiple, non-consecutive tokens in parallel. SBD avoids the complexity of auxiliary models and complex architectural constructions and requires no architectural changes, making it a practical solution that can be readily implemented by fine-tuning existing language models. Our experiments with Llama-3.1 8B and Qwen-3 8B demonstrate that SBD reduces the number of required forward passes by 3x-5x without compromising the model’s original performance.

There are several interesting directions for future work. A key direction is scaling SBD to even larger models to investigate its scaling properties. Furthermore, developing hardware-aware inference implementations to match the theoretical roofline analysis, as well as exploring a wider range of advanced samplers from the discrete diffusion literature, could further unlock the potential of SBD to maximize wall-clock speedups.

## 7 Acknowledgements

We thank Shimon Nowik for his contributions to the method’s visualizations and Grigory Sizov for his support with the practical implementation.

## References

Wasi Uddin Ahmad, Sean Narenthiran, Somshubra Majumdar, Aleksander Ficek, Siddhartha Jain, Jocelyn Huang, Vahid Noroozi, and Boris Ginsburg. Opencodereasoning: Advancing data distillation for competitive coding. 2025.

Marianne Arriola, Aaron Gokaslan, Justin T Chiu, Zhihan Yang, Zhixuan Qi, Jiaqi Han, Subham Sekhar Sahoo, and Volodymyr Kuleshov. Block diffusion: Interpolating between autoregressive and diffusion language models. *arXiv preprint arXiv:2503.09573*, 2025.

Jacob Austin, Augustus Odena, Maxwell Nye, Maarten Bosma, Henryk Michalewski, David Dohan, Ellen Jiang, Carrie Cai, Michael Terry, Quoc Le, et al. Program synthesis with large language models. *arXiv preprint arXiv:2108.07732*, 2021.

Heli Ben-Hamu, Itai Gat, Daniel Severo, Niklas Nolte, and Brian Karrer. Accelerated sampling from masked diffusion models via entropy bounded unmasking. *arXiv preprint arXiv:2505.24857*, 2025.

Tianle Cai, Yuhong Li, Zhengyang Geng, Hongwu Peng, Jason D Lee, Deming Chen, and Tri Dao. Medusa: Simple llm inference acceleration framework with multiple decoding heads. *arXiv preprint arXiv:2401.10774*, 2024.

Charlie Chen, Sebastian Borgeaud, Geoffrey Irving, Jean-Baptiste Lespiau, Laurent Sifre, and John Jumper. Accelerating large language model decoding with speculative sampling. *arXiv preprint arXiv:2302.01318*, 2023.

Jacob K Christopher, Brian R Bartoldson, Tal Ben-Nun, Michael Cardei, Bhavya Kailkhura, and Ferdinando Fioretto. Speculative diffusion decoding: Accelerating language generation through diffusion, 2025. <https://arxiv.org/abs/2408.05636>.

Peter Clark, Isaac Cowhey, Oren Etzioni, Tushar Khot, Ashish Sabharwal, Carissa Schoenick, and Oyvind Tafjord. Think you have solved question answering? try arc, the ai2 reasoning challenge. *ArXiv*, abs/1803.05457, 2018.

Karl Cobbe, Vineet Kosaraju, Mohammad Bavarian, Mark Chen, Heewoo Jun, Lukasz Kaiser, Matthias Plappert, Jerry Tworek, Jacob Hilton, Reiichiro Nakano, Christopher Hesse, and John Schulman. Training verifiers to solve math word problems, 2021. <https://arxiv.org/abs/2110.14168>.

Tri Dao, Daniel Y. Fu, Stefano Ermon, Atri Rudra, and Christopher Ré. FlashAttention: Fast and memory-efficient exact attention with IO-awareness. In *Advances in Neural Information Processing Systems (NeurIPS)*, 2022.

Google Deepmind. Gemini diffusion, 2025. <https://deepmind.google/models/gemini-diffusion/>.

Juechu Dong, Boyuan Feng, Driss Guessous, Yanbo Liang, and Horace He. Flex attention: A programming model for generating optimized attention kernels, 2024. <https://arxiv.org/abs/2412.05496>.

Nima Fathi, Torsten Scholak, and Pierre-André Noël. Unifying autoregressive and diffusion-based sequence generation, 2025. <https://arxiv.org/abs/2504.06416>.

Itai Gat, Tal Remez, Neta Shaul, Felix Kreuk, Ricky TQ Chen, Gabriel Synnaeve, Yossi Adi, and Yaron Lipman. Discrete flow matching. *Advances in Neural Information Processing Systems*, 37:133345–133385, 2024.

Marjan Ghazvininejad, Omer Levy, Yinhan Liu, and Luke Zettlemoyer. Mask-predict: Parallel decoding of conditional masked language models. *arXiv preprint arXiv:1904.09324*, 2019.

Fabian Gloeckle, Badr Youbi Idrissi, Baptiste Rozière, David Lopez-Paz, and Gabriel Synnaeve. Better & faster large language models via multi-token prediction. *arXiv preprint arXiv:2404.19737*, 2024.

Shansan Gong, Ruixiang Zhang, Huangjie Zheng, Jiatao Gu, Navdeep Jaitly, Lingpeng Kong, and Yizhe Zhang. Diffucoder: Understanding and improving masked diffusion models for code generation, 2025. <https://arxiv.org/abs/2506.20639>.

Gabe Guo and Stefano Ermon. Reviving any-subset autoregressive models with principled parallel sampling and speculative decoding. *arXiv preprint arXiv:2504.20456*, 2025.

Dan Hendrycks, Collin Burns, Steven Basart, Andy Zou, Mantas Mazeika, Dawn Song, and Jacob Steinhardt. Measuring massive multitask language understanding. *Proceedings of the International Conference on Learning Representations (ICLR)*, 2021.

Emiel Hoogeboom, Alexey A. Gritsenko, Jasmijn Bastings, Ben Poole, Rianne van den Berg, and Tim Salimans. Autoregressive diffusion models. In *International Conference on Learning Representations*, 2022. <https://openreview.net/forum?id=Lm8T39vLDTE>.

Zhanqiu Hu, Jian Meng, Yash Akhauri, Mohamed S Abdelfattah, Jae-sun Seo, Zhiru Zhang, and Udit Gupta. Accelerating diffusion language model inference via efficient kv caching and guided diffusion. *arXiv preprint arXiv:2505.21467*, 2025.

Chihang Huang and Hao Tang. Ctrldiff: Boosting large diffusion language models with dynamic block prediction and controllable generation, 2025. <https://arxiv.org/abs/2505.14455>.

Daniel Israel, Guy Van den Broeck, and Aditya Grover. Accelerating diffusion llms via adaptive parallel decoding. *arXiv preprint arXiv:2506.00413*, 2025.

Naman Jain, King Han, Alex Gu, Wen-Ding Li, Fanjia Yan, Tianjun Zhang, Sida Wang, Armando Solar-Lezama, Koushik Sen, and Ion Stoica. Livecodebench: Holistic and contamination free evaluation of large language models for code. *arXiv preprint arXiv:2403.07974*, 2024.

Inception Labs, Samar Khanna, Siddhant Kharbanda, Shufan Li, Harshit Varma, Eric Wang, Sawyer Birnbaum, Ziyang Luo, Yanis Miraoui, Akash Palrecha, Stefano Ermon, Aditya Grover, and Volodymyr Kuleshov. Mercury: Ultra-fast language models based on diffusion, 2025. <https://arxiv.org/abs/2506.17298>.

Yaniv Leviathan, Matan Kalman, and Yossi Matias. Fast inference from transformers via speculative decoding. In *International Conference on Machine Learning*, pages 19274–19286. PMLR, 2023.

Jeffrey Li, Alex Fang, Georgios Smyrnis, Maor Ivgi, Matt Jordan, Samir Gadre, Hritik Bansal, Etash Guha, Sedrick Keh, Kushal Arora, Saurabh Garg, Rui Xin, Niklas Muennighoff, Reinhard Heckel, Jean Mercat, Mayee Chen, Suchin Gururangan, Mitchell Wortsman, Alon Albalak, Yonatan Bitton, Marianna Nezhurina, Amro Abbas, Cheng-Yu Hsieh, Dhruba Ghosh, Josh Gardner, Maciej Kilian, Hanlin Zhang, Rulin Shao, Sarah Pratt, Sunny Sanyal, Gabriel Ilharco, Giannis Daras, Kalyani Marathe, Aaron Gokaslan, Jieyu Zhang, Khyathi Chandu, Thao Nguyen, Igor Vasiljevic, Sham Kakade, Shuran Song, Sujay Sanghavi, Fartash Faghri, Sewoong Oh, Luke Zettlemoyer, Kyle Lo, Alaaeldin El-Nouby, Hadi Pouransari, Alexander Toshev, Stephanie Wang, Dirk Groeneveld, Luca Soldaini, Pang Wei Koh, Jenia Jitsev, Thomas Kollar, Alexandros G. Dimakis, Yair Carmon, Achal Dave, Ludwig Schmidt, and Vaishaal Shankar. Datacomp-lm: In search of the next generation of training sets for language models, 2024a.

Yuhui Li, Fangyun Wei, Chao Zhang, and Hongyang Zhang. Eagle: Speculative sampling requires rethinking feature uncertainty. In *International Conference on Machine Learning*, pages 28935–28948. PMLR, 2024b.

Hunter Lightman, Vineet Kosaraju, Yura Burda, Harri Edwards, Bowen Baker, Teddy Lee, Jan Leike, John Schulman, Ilya Sutskever, and Karl Cobbe. Let’s verify step by step. *arXiv preprint arXiv:2305.20050*, 2023.

Jiawei Liu, Chunqiu Steven Xia, Yuyao Wang, and Lingming Zhang. Is your code generated by chatGPT really correct? rigorous evaluation of large language models for code generation. In *Thirty-seventh Conference on Neural Information Processing Systems*, 2023. <https://openreview.net/forum?id=1qvxf610Cu7>.

Xiaoran Liu, Zhigeng Liu, Zengfeng Huang, Qipeng Guo, Ziwei He, and Xipeng Qiu. Longllada: Unlocking long context capabilities in diffusion llms, 2025a. <https://arxiv.org/abs/2506.14429>.

Zhiyuan Liu, Yicun Yang, Yaojie Zhang, Junjie Chen, Chang Zou, Qingyuan Wei, Shaobo Wang, and Linfeng Zhang. dilm-cache: Accelerating diffusion large language models with adaptive caching, 2025b. <https://arxiv.org/abs/2506.06295>.

Ilya Loshchilov and Frank Hutter. Decoupled weight decay regularization, 2019. <https://arxiv.org/abs/1711.05101>.

Aaron Lou, Chenlin Meng, and Stefano Ermon. Discrete diffusion modeling by estimating the ratios of the data distribution. *arXiv preprint arXiv:2310.16834*, 2023.

Xinyin Ma, Runpeng Yu, Gongfan Fang, and Xinchao Wang. dkv-cache: The cache for diffusion language models. *arXiv preprint arXiv:2505.15781*, 2025.

Llama 3 Team Meta. The llama 3 herd of models, 2024. <https://arxiv.org/abs/2407.21783>.

Ivan Moshkov, Darragh Hanley, Ivan Sorokin, Shubham Toshniwal, Christof Henkel, Benedikt Schifferer, Wei Du, and Igor Gitman. Aimo-2 winning solution: Building state-of-the-art mathematical reasoning models with openmath reasoning dataset. *arXiv preprint arXiv:2504.16891*, 2025.

Shen Nie, Fengqi Zhu, Zebin You, Xiaolu Zhang, Jingyang Ou, Jun Hu, Jun Zhou, Yankai Lin, Ji-Rong Wen, and Chongxuan Li. Large language diffusion models. *arXiv preprint arXiv:2502.09992*, 2025.

Arnaud Pannatier, Evann Courdier, and François Fleuret.  $\sigma$ -gpts: A new approach to autoregressive models. In *Joint European Conference on Machine Learning and Knowledge Discovery in Databases*, pages 143–159. Springer, 2024.

David Rein, Betty Li Hou, Asa Cooper Stickland, Jackson Petty, Richard Yuanzhe Pang, Julien Dirani, Julian Michael, and Samuel R. Bowman. Gpqa: A graduate-level google-proof q&a benchmark, 2023.

Subham Sekhar Sahoo, Zhihan Yang, Yash Akhauri, Johnna Liu, Deepansha Singh, Zhoujun Cheng, Zhengzhong Liu, Eric Xing, John Thickstun, and Arash Vahdat. Esoteric language models. *arXiv preprint arXiv:2506.01928*, 2025.

Keisuke Sakaguchi, Ronan Le Bras, Chandra Bhagavatula, and Yejin Choi. Winogrande: An adversarial winograd schema challenge at scale. *arXiv preprint arXiv:1907.10641*, 2019.

Jiaxin Shi, Kehang Han, Zhe Wang, Arnaud Doucet, and Michalis Titsias. Simplified and generalized masked diffusion for discrete data. *Advances in neural information processing systems*, 37:103131–103167, 2024.

Yuxuan Song, Zheng Zhang, Cheng Luo, Pengyang Gao, Fan Xia, Hao Luo, Zheng Li, Yuehang Yang, Hongli Yu, Xingwei Qu, Yuwei Fu, Jing Su, Ge Zhang, Wenhao Huang, Mingxuan Wang, Lin Yan, Xiaoying Jia, Jingjing Liu, Wei-Ying Ma, Ya-Qin Zhang, Yonghui Wu, and Hao Zhou. Seed diffusion: A large-scale diffusion language model with high-speed inference, 2025. <https://arxiv.org/abs/2508.02193>.

Mitchell Stern, Noam Shazeer, and Jakob Uszkoreit. Blockwise parallel decoding for deep autoregressive models. *Advances in Neural Information Processing Systems*, 31, 2018.

Benigno Uria, Iain Murray, and Hugo Larochelle. A deep and tractable density estimator. In Eric P. Xing and Tony Jebara, editors, *Proceedings of the 31st International Conference on Machine Learning*, volume 32 of *Proceedings of Machine Learning Research*, pages 467–475, Bejing, China, 22–24 Jun 2014. PMLR.

Samuel Webb Williams, Andrew Waterman, and David A Patterson. Roofline: An insightful visual performance model for floating-point programs and multicore architectures. Technical report, Technical Report UCB/EECS-2008-134, EECS Department, University of . . . . ., 2008.

Chengyue Wu, Hao Zhang, Shuchen Xue, Zhijian Liu, Shizhe Diao, Ligeng Zhu, Ping Luo, Song Han, and Enze Xie. Fast-dllm: Training-free acceleration of diffusion llm by enabling kv cache and parallel decoding. *arXiv preprint arXiv:2505.22618*, 2025a.

Zirui Wu, Lin Zheng, Zhihui Xie, Jiacheng Ye, Jiahui Gao, Yansong Feng, Zhenguo Li, Victoria W., Guorui Zhou, and Lingpeng Kong. Dreamon: Diffusion language models for code infilling beyond fixed-size canvas, 2025b. <https://hkunlp.github.io/blog/2025/dreamon>.

Zhihui Xie, Jiacheng Ye, Lin Zheng, Jiahui Gao, Jingwei Dong, Zirui Wu, Xueliang Zhao, Shansan Gong, Xin Jiang, Zhenguo Li, and Lingpeng Kong. Dream-coder 7b, 2025. <https://hkunlp.github.io/blog/2025/dream-coder>.

An Yang, Anfeng Li, Baosong Yang, Beichen Zhang, Binyuan Hui, Bo Zheng, Bowen Yu, Chang Gao, Chengen Huang, Chenxu Lv, Chujie Zheng, Dayiheng Liu, Fan Zhou, Fei Huang, Feng Hu, Hao Ge, Haoran Wei, Huan Lin, Jialong Tang, Jian Yang, Jianhong Tu, Jianwei Zhang, Jianxin Yang, Jiaxi Yang, Jing Zhou, Jingren Zhou, Junyang Lin, Kai Dang, Keqin Bao, Kexin Yang, Le Yu, Lianghao Deng, Mei Li, Mingfeng Xue, Mingze Li, Pei Zhang, Peng Wang, Qin Zhu, Rui Men, Ruize Gao, Shixuan Liu, Shuang Luo, Tianhao Li, Tianyi Tang, Wenbiao Yin, Xingzhang Ren, Xinyu Wang, Xinyu Zhang, Xuancheng Ren, Yang Fan, Yang Su, Yichang Zhang, Yinger Zhang, Yu Wan, Yuqiong Liu, Zekun Wang, Zeyu Cui, Zhenru Zhang, Zhipeng Zhou, and Zihan Qiu. Qwen3 technical report, 2025a. <https://arxiv.org/abs/2505.09388>.

Ling Yang, Ye Tian, Bowen Li, Xinchen Zhang, Ke Shen, Yunhai Tong, and Mengdi Wang. Mmada: Multimodal large diffusion language models, 2025b. <https://arxiv.org/abs/2505.15809>.

Zebin You, Shen Nie, Xiaolu Zhang, Jun Hu, Jun Zhou, Zhiwu Lu, Ji-Rong Wen, and Chongxuan Li. Llada-v: Large language diffusion models with visual instruction tuning. *arXiv preprint arXiv:2505.16933*, 2025.

Runpeng Yu, Xinyin Ma, and Xinchao Wang. Dimple: Discrete diffusion multimodal large language model with parallel decoding. *arXiv preprint arXiv:2505.16990*, 2025.

Rowan Zellers, Ari Holtzman, Yonatan Bisk, Ali Farhadi, and Yejin Choi. Hellaswag: Can a machine really finish your sentence? In *Proceedings of the 57th Annual Meeting of the Association for Computational Linguistics*, 2019.

# Appendix

## A Implementation

### A.1 Method

The following PyTorch snippets highlight the key modifications for our method, focusing on the changes to a standard autoregressive framework. Code Block 7 presents the adjustments to the training loop required to learn a hybrid model. The subsequent code blocks detail our custom attention mechanism, implemented using FlexAttention (Dong et al., 2024): code block 9 for training and code block 10 for inference.

```
1  input_ids = sequence[:, :-1]
2
3  ar_label_ids = sequence[:, 1:]
4  parallel_label_ids = input_ids.clone()
5
6  bsz, seq_len = input_ids.shape
7
8  block_len = torch.randint(max_block_size, (1, )).item()
9  attention_mask = create_attention_mask_train(seq_len=seq_len, block_len=block_len)
10
11 # 1. Compute masked_input
12 time = torch.rand(size=(bsz, 1), device="cuda")
13 input_ids_mask = torch.rand(size=input_ids.shape, device=input_ids.device) > time
14
15 masked_input = torch.where(condition=input_ids_mask, input=tokenizer.mask_id, other=input_ids)
16
17 input_ids = torch.cat([input_ids, masked_input], dim=1)
18
19 # 2. Compute label_ids
20 parallel_label_ids[:, :-1][input_ids_mask] = -100
21
22 label_ids = torch.cat([ar_label_ids, parallel_label_ids], dim=1)
23
24 # 3. Each unique token location (in AR and parallel) should get the same positional embeddings.
25 positional_embeddings = get_positional_embeddings(seq_len=seq_len)
26 positional_embeddings = positional_embeddings.repeat(2, 1)
27
28 loss = model(input_ids, mask=attention_mask, targets=label_ids, positional_embeddings=positional_embeddings)
29 loss.backward()
30
31 ...
```

**Figure 7** The required modifications to the training loop of an autoregressive model. We first change how the attention mask is computed, then mask a portion of the input tokens. The block-length is chosen randomly.

Input	Target	$x_1$	$x_2$	$x_3$	$x_4$	$x_1$	m	$x_3$	m	$x_5$	$x_6$	$x_7$	$x_8$	m	m	$x_7$	m
$x_1$	$x_2$																
$x_2$	$x_3$																
$x_3$	$x_4$																
$x_4$	$x_5$																
$x_1$	-																
m	$x_2$																
$x_3$	-																
m	$x_4$																
$x_5$	$x_6$																
$x_6$	$x_7$																
$x_7$	$x_8$																
$x_8$	$x_9$																
m	$x_5$																
m	$x_6$																
$x_7$	-																
m	$x_8$																

**Figure 8** Training a hybrid model for block of size  $k = 4$ . We show input tokens (left column), target tokens used for Cross-Entropy loss (second columns) and attention matrix.

```

1  from torch.nn.attention.flex_attention import BlockMask, create_block_mask
2
3  def create_attention_mask_train(seq_len: int, block_len: int) -> BlockMask:
4      half_seq_len: int = seq_len // 2
5
6      def mask_mod(b, h, q_idx, kv_idx):
7          # Top-left quadrant (x1 -> x1, standard causal)
8          # True if query and key are in the first half and key is before or at query.
9          is_in_top_left_causal = (q_idx < half_seq_len) & (kv_idx < half_seq_len) & (kv_idx <= q_idx)
10
11         # Bottom-right quadrant (xt -> xt, block attention)
12         # True if query and key are in the second half and belong to the same block.
13         q_block_xt = (q_idx - half_seq_len) // block_len
14         kv_block_xt = (kv_idx - half_seq_len) // block_len
15         is_in_bottom_right_block = (q_idx >= half_seq_len) & (kv_idx >= half_seq_len) & (q_block_xt ==
16             kv_block_xt)
17
18         # Bottom-left quadrant (xt -> x1, block causal past)
19         # True if query is in the second half, key is in the first half, and the queries block index is
20             # strictly greater than the keys block index.
21         q_block_idx_bl = (q_idx - half_seq_len) // block_len
22         kv_block_idx_bl = kv_idx // block_len
23         is_in_bottom_left_block_causal_past = (q_idx >= half_seq_len) & (kv_idx < half_seq_len) &
24             (q_block_idx_bl > kv_block_idx_bl)
25
26     return is_in_top_left_causal | is_in_bottom_right_block | is_in_bottom_left_block_causal_past
27
28     return create_block_mask(mask_mod, B=None, H=None, Q_LEN=seq_len, KV_LEN=seq_len)

```

**Figure 9** FlexAttention implementation of the attention mask at training time (see figure 8 for a visual representation).

```
1  from torch.nn.attention.flex_attention import BlockMask, create_block_mask
2
3  def create_attention_mask_inference(causal_point: int) -> BlockMask:
4      # causal_point is the index of the first token in the prediction block
5      def mask_mod(b, h, q_idx, kv_idx):
6          is_causal = (kv_idx <= q_idx)
7          is_past_causal_point = (causal_point <= q_idx)
8          return is_causal | is_past_causal_point
9      return create_block_mask(mask_mod, B=None, H=None, Q_LEN=seq_len, KV_LEN=seq_len)
```

**Figure 10** FlexAttention implementation of the attention mask at inference time. The attention is causal up until the point where the prediction block begins. The tokens in the prediction block attend to all other tokens in the sequence.

## A.2 Roofline model

```

1 def gemm_roofline(m: int, n: int, k: int) -> tuple[float, float]:
2     "Returns the runtime (in s) and flops of doing a `C=A@B` with A/B of shape `[m, k]/[k, n]`"
3     total_IO = (
4         m * k * BYTES + # read A
5         n * k * BYTES + # read B
6         m * n * BYTES   # write C
7     )
8     total_flops = 2 * m * n * k
9     return max(total_IO / MEMORY_BANDWIDTH, total_flops / PEAK_FLOPS), total_flops
10
11 # Attention roofline analysis
12 def calculate_fused_attention_roofline(block_size: int, kv_length: int, batch_size: int) -> float:
13     num_tokens = block_size * batch_size
14     # Memory in Q: (batch_size, block_size, NUM_HEADS, HEAD_DIM)
15     bytes_Q = num_tokens * NUM_HEADS * HEAD_DIM * BYTES
16     # Memory in K: (batch_size, kv_length, NUM_KV_HEADS, HEAD_DIM)
17     bytes_K = batch_size * kv_length * NUM_KV_HEADS * HEAD_DIM * BYTES_PER_KV_ELEMENT
18     # Flops P=QK^T
19     _, flops_QKt = gemm_roofline(num_tokens, kv_length, NUM_HEADS * HEAD_DIM)
20     # Softmax memory transfer is ignored as it's not read or stored in memory, flops negligible
21     bytes_softmax = 0
22     # Memory in V: (batch_size, kv_length, NUM_KV_HEADS, HEAD_DIM)
23     bytes_V = batch_size * kv_length * NUM_KV_HEADS * HEAD_DIM * BYTES_PER_KV_ELEMENT
24     # Flops PV
25     _, flops_PV = gemm_roofline(num_tokens, kv_length, NUM_HEADS * HEAD_DIM)
26     # Memory out PV: (batch_size, block_size, NUM_HEADS, HEAD_DIM)
27     bytes_PV = num_tokens * NUM_HEADS * HEAD_DIM * BYTES
28
29     total_memory = bytes_Q + bytes_K + bytes_V + bytes_PV + bytes_softmax
30     total_flops = flops_QKt + flops_PV
31     return max(total_memory / MEMORY_BANDWIDTH, total_flops / PEAK_FLOPS_ATTENTION)
32
33
34 # FFN roofline analysis
35 def calculate_linear_layers_roofline(block_size: int, batch_size: int) -> float:
36     num_tokens = block_size * batch_size
37     # FFN: Up-projection
38     total_time = gemm_roofline(num_tokens, HIDDEN_DIM, HIDDEN_DIM * FFN_DIM)[0]
39     # FFN: Down-projection
40     total_time += gemm_roofline(num_tokens, HIDDEN_DIM * FFN_DIM, HIDDEN_DIM)[0]
41     # Attention linear layers
42     total_time += gemm_roofline(num_tokens, HIDDEN_DIM, NUM_HEADS * HEAD_DIM)[0] # Q-proj
43     total_time += gemm_roofline(num_tokens, HIDDEN_DIM, NUM_HEADS * NUM_KV_HEADS)[0] # K-proj
44     total_time += gemm_roofline(num_tokens, HIDDEN_DIM, NUM_HEADS * NUM_KV_HEADS)[0] # V-proj
45     total_time += gemm_roofline(num_tokens, NUM_HEADS * HEAD_DIM, HIDDEN_DIM)[0] # out-proj
46     return total_time

```

**Figure 11** Transformer roofline analysis.

## B Additional experiments

### B.1 Sampling algorithm

In all our experiments we used EB-Sampler in its simplest form with entropy error proxy (see [equation 8](#)). In this section we ablate on two other sampling variants: (i) Factor parallel decoding ([Wu et al., 2025a](#)); and (ii) EB-Sampler with confidence error proxy ([Ben-Hamu et al., 2025](#)). For completeness, let us briefly describe the two.

Recently, [Wu et al. \(2025a\)](#) proposed the Factor parallel decoding approach for sampling. With a similar motivation as the EB-Sampler, the Factor method proposes an adaptive parallel decoding algorithm that in high confidence regimes is equivalent to greedy decoding. At each step, given we already decoded the tokens in indices  $\mathcal{J} \subset \mathcal{I}$  and are left with masks  $\mathcal{M} = \mathcal{I} \setminus \mathcal{J}$ , compute the confidence for each masked index  $c^i = \max_{x_i \in \mathcal{V}} p(x_i | x_{<t}, x_{\mathcal{J}}), i \in \mathcal{M}$ , sort the masked indices by confidence  $i_1, i_2, \dots, i_{|\mathcal{M}|}$  and unmask the  $n$  first tokens. Where  $n$  is the largest such that  $(n+1)c^n < f$  and  $f$  is a predefined threshold hyperparameter. In [figure 12](#) we compare the performance of the EB-Sampler with entropy error proxy to the factor method on the 3B SFT models from [section 3.2](#). EB-Sampler with entropy error proxy compares favorably to the Factor method on HumanEval at all training budgets, where on MBPP and GSM8K both approaches perform similarly when models are trained for more steps.

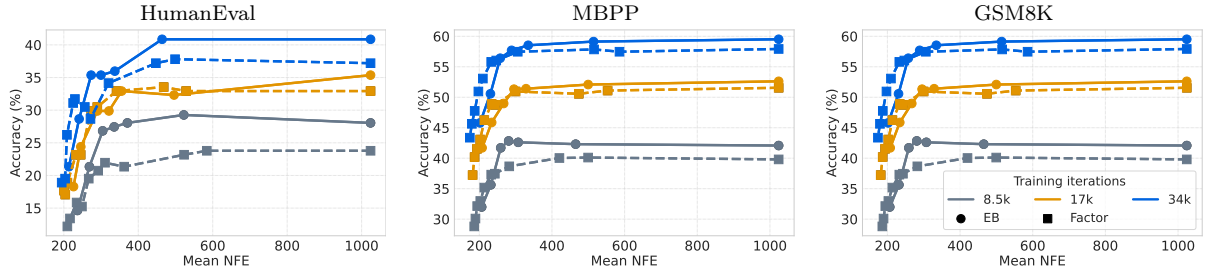


**Figure 12** 3B model SFT training with varying number of training steps. Factor vs EB-Sampler with entropy error proxy.

Interestingly, the Factor method is more closely related to the EB-Sampler instance that uses confidence as an error proxy. In each step this instance sorts the masked tokens,  $\mathcal{M}$ , by confidence, similarly to the Factor method, but chooses how many to unmask according to the entropy bound on the mutual information, finding the largest  $s$  such that:

$$\sum_{j=1}^s H(p(x_{i_j} | x_{<t}, x_{\mathcal{J}})) - \max_{j' \leq s} H(p(x_{i_{j'}} | x_{<t}, x_{\mathcal{J}})) \leq \gamma, \quad (18)$$

[Figure 13](#) shows the performance of the EB-Sampler with confidence error proxy compared to the Factor method at different  $\gamma$  and  $f$  values respectively, empirically demonstrating the similarity of the two approaches. Notably, [figure 12](#) and [figure 13](#) also show that entropy as an error proxy compares favorably for the tested models. The models used in this experiment are again the 3B SFT models from [section 3.2](#).

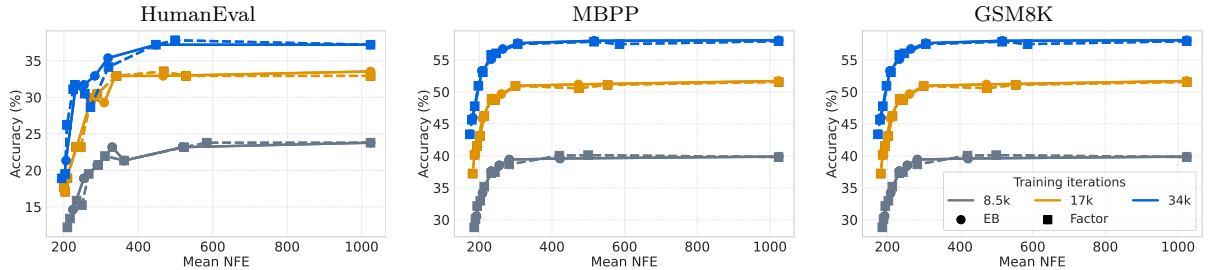


**Figure 13** 3B model SFT training with varying number of training steps. Factor vs EB-Sampler with confidence error proxy.